# A Method to Upgrade Iceberg Velocity Statistics to Include Wave-Induced Motion

**J. H. Lever**

**D. Sen**

Faculty of Engineering and Applied Science,
Memorial University of Newfoundland,
St. John's, Newfoundland, Canada

*Iceberg impact design loads for offshore structures can be estimated by incorporating an ice/structure interaction model in a probabilistic framework, or risk analysis. The relevant iceberg and environmental parameters are input in statistical form. Iceberg velocity statistics are usually compiled from drilling rig radar reports, and hence represent estimates of average hourly drift speeds. Yet it is the instantaneous ice velocity which is the relevant input to the simulation of the iceberg/structure collision process. Thus, risk analyses based on mean drift speed distributions will only yield valid results for the subset of conditions where wave-induced iceberg motion is negligible. This paper describes a method which, for the first time, systematically accounts for wave-induced motion in iceberg impact risk analyses. A linear three-dimensional potential flow model is utilized to upgrade iceberg velocity statistics to include the influence of Grand Banks sea-state conditions on instantaneous ice motion. The results clearly demonstrate the importance of including wave-induced motion in iceberg impact risk analyses.*

## 1 Introduction

Petroleum exploration and production operations in the Labrador Sea and Grand Banks regions face a unique environmental hazard: the possible collision of an iceberg with an offshore structure. Substantial efforts are underway to determine the loading on, and deformation of, various offshore structure designs in the event of such a collision, e.g., [1–3]. For a given set of initial conditions (iceberg size, shape, initial velocity, mechanical properties, structural geometry, material properties, dynamic characteristics, etc.), these models produce estimates of the maximum load experienced by the structure during the collision, and the degree of structural damage sustained. In order to determine the maximum impact load a structure should be designed to withstand during its life span, an iceberg/structure impact model is incorporated into a probabilistic framework known as risk analysis. These risk analyses account for the random nature of the iceberg collision hazard via statistical representations of the input conditions, specifically those related to the iceberg. In this way, an estimation of iceberg impact load as a function of probability of occurrence is obtained. To design for a given level of acceptable risk, the estimated impact load for that risk is obtained, and the structure is designed to withstand that load within an appropriate factor of safety.

Many such risk analyses have been formulated for iceberg/structure interactions, e.g., [4–6]. The statistical representations for the iceberg initial conditions are normally obtained from available full-scale observations. One such representation, for iceberg velocity statistics, is the subject of the present work.

Contributed by the OMAE Division for publication in the JOURNAL OF OFFSHORE MECHANICS AND ARCTIC ENGINEERING. Manuscript received by the OMAE Division, October 24, 1986.

The compilation of iceberg velocity statistics has been based essentially on drilling rig radar trackings, with range and bearing of iceberg targets recorded at hourly intervals, e.g., [7–9]. This procedure produces estimates of average hourly drift speeds of icebergs, and excludes velocity variations on shorter time scales due to ocean waves. However, instantaneous ice velocity is the relevant input to the simulation of the iceberg/structure collision process. Risk analyses based on mean drift speed distributions will underestimate impact velocities for small ice masses in waves. Conversely, risk analyses which apply a uniform increase in iceberg speeds regardless of mass, such as that by Johnson and Nevel [6], will tend to overestimate impact velocities for large bergs.

Previous wave tank work by Lever et al. [10] suggests that instantaneous velocites of small icebergs, bergy bits and growlers in typical Grand Banks storm waves can substantially exceed maximum expected mean drift speeds. Since the combination of ice and heavy seas at a given rig site might be considered a rare event, it makes sense to investigate the influence of various sea states on ice masses of various sizes to determine under what conditions wave-induced motion becomes significant. That is, if instantaneous ice velocity distributions can be obtained as functions of berg size and sea-state conditions, then these may be combined with available sea-state statistics and iceberg size frequency distributions to determine to what degree impact design loads are affected by the phenomenon of wave-induced motion.

While the motion response to waves of ice floes and large Antarctic icebergs has been studied, e.g., [11–13], the influence of waves on instantaneous iceberg and bergy-bit motion has not received systematic attention. Hsiung and Aboul-Azim [14] investigated the second-order steady drift force exerted by waves on a small iceberg; Lever, et al. [10] con-

ducted a wave tank study of various model ice sizes and shapes to determine maximum instantaneous velocities in storm waves; a field program to directly measure instantaneous iceberg motion has been initiated by Lever and Diemand [15]. A need still exists to determine in a systematic way the importance of wave effects on iceberg motion over broad ranges of ice sizes and sea-states.

Described in this paper is a new method which allows the phenomenon of wave-induced motion to be systematically taken into account in iceberg impact risk analyses. A linear, three-dimensional wave diffraction model is employed to compute the surge and heave responses to linear waves of five blocky icebergs, bergy bits and growlers. The surge responses of the ice masses in random unidirectional seas are then obtained, with the significant surge velocity expressed as function of significant wave height for each berg simulated. The probability densities for instantaneous surge velocities are then obtained from sea-state probabilities for the Grand Banks. Finally, the total velocity probability distribution for each ice mass is computed by combining existing drift speed probabilities with the newly computed instantaneous surge velocity distributions. The resulting total velocity probability densities may then be used as input for risk analyses. This will give a better representation of the broad range of initial conditions relevant to iceberg/structure interactions, particularly those conditions involving relatively small ice masses in heavy seas where mean velocities alone severely underestimate the impact hazard.

## 2 Wave-Induced Velocity as Function of Ice Size and Sea-State

**2.1 Theoretical Model for Oscillatory Motion Response.** Computation of the motion response of an iceberg is based here on linearized potential flow theory. The flow is assumed to be inviscid, irrotational and incompressible, such that the flow field can be characterized by a single-valued velocity potential. This potential is composed of the incident wave potential, plus the diffraction potential produced by the stationary body, plus the six radiation potentials arising from the oscillatory motion of the body about its equilibrium position in still fluid. The unknown amplitudes of oscillation in the six rigid body degrees-of-freedom are obtained for a given unit amplitude input wave at a known frequency by proper matching of boundary conditions. Linear superposition is then used to obtain the motion responses in random sea conditions.

The key assumptions necessary to apply linear potential flow theory are that viscous effects are negligible, incident wave steepness is small, and body motion is small. For large bodies, it is felt that viscous effects are confined to the boundary layer on the body and local separated flow regions, without significantly affecting the overall flow field [16]. Potential flow theory has been used to compute the motion of floating bodies, e.g., [16–19] and large ice floes and icebergs in waves [11–13]. For the case of bergy bits and growlers in waves, the role of fluid viscosity is less well understood, as these bodies will in general not be large relative to the constitutive wavelengths in a random sea. However, the assumption of inviscid, irrotational flow is applied to make the problem tractable.

A similar situation exists for the linearizing assumptions of small wave steepness and small body motion. For small bergy bits and growlers in heavy seas, the amplitudes of motion will approach the wave amplitudes. Also, in heavy seas, wave steepnesses do not remain small, with breaking waves a definite possibility. The authors are currently working on a nonlinear potential flow theory to model the large amplitude motion of small ice masses in steep waves. The importance of fluid viscosity will be studied simultaneously in the wave tank. The linear potential flow theory presented here is felt to be the most appropriate means at the current time to investigate the broad range of ice sizes and sea states relevant to the problem, and the method easily lends itself to a probabilistic formulation.

A three-dimensional singularity distribution (or Green's function) method has been used to compute the wave-induced motion response of idealized icebergs. The foundation of this method was first established by Kim [20], and was later extended and applied to various bodies by Garrison [18] and Faltinsen and Michelsen [17]. Since then, the effectiveness, reliability and accuracy of this method has been demonstrated extensively, e.g., [21–24]. This method is felt to be the most versatile technique for the computation of small-amplitude oscillatory motion of large floating bodies of arbitrary geometry in a potential flow field. The main drawback of the method is the large computational effort required compared to methods dealing with restricted classes of bodies (e.g., slender bodies or vessels, bodies with planes or axes of symmetry).

A complete description of the three-dimensional singularity distribution technique may be found in reference [24]. The mean wetted body surface is discretized by a number of surface panels. The first-order velocity potential is solved numerically by distributing sources at the centroid of each panel and applying the linearized boundary conditions. The program has been checked with several published results and, in general, good agreement is found [24]. Comparisons of computed response amplitude operators with available published results for cylindrical and cubical floating bodies are shown in Figs. 1 and 2.

**2.2 Response of Idealized Icebergs to Regular Waves.** Cubical shapes were chosen to represent the icebergs for the purposes of this study. This was considered acceptable for a first attempt, since the aims were to develop a method for, and assess the importance of, including wave-induced motion in iceberg/structure impact risk analyses. The potential flow model may be applied to arbitrarily shaped floating bodies, so that extension of the work to more realistic iceberg shapes is straightforward.

The icebergs were treated as being homogenous, with a density of 900 kg/m$^3$. The five cubical bergs had masses of 1600, 12,000, 42,000, 100,000 and 1,000,000 tonnes, with corresponding side lengths of 12, 24, 36, 48, 104 m, respectively. The density of sea water was taken to be 1025 kg/m$^3$ uniformly. The water depth used was 90 m for all cases except the 1 million-ton iceberg, where a value of 180 m was chosen to accommodate the deep draft of this berg.

All icebergs were discretized using 80 surface panels. This value was felt to be sufficient, as previous investigation of a 90 × 90 × 20-m floating box indicated that 48 panels were sufficient to produce accurate results [24].

The computed response amplitude operators (RAOs) for surge (forward) and heave (vertical) motions are shown in Figs. 3 and 4, respectively. These represent, for each model iceberg, the nondimensional amplitude of the sinusoidal response to regular waves at various periods. Only surge and heave RAOs are shown, as these are the motions of greatest concern in iceberg/structure impact analyses. These response curves show similar behavior to those obtained for other blocky floating bodies, e.g., [11, 12, 23].

An interesting comparison with earlier work is possible at this stage. Experimental results obtained by Lever, et al. [10] indicated that motion if iceberg models in regular steep waves tended toward fluid particlelike motion for values of wavelength to model size ratio greater than 13. To investigate this effect, ratios of surge and heave velocity amplitudes to horizontal and vertical particle velocity amplitudes, respectively, $V_{\text{surge}}/U_{\text{horizontal}}$ and $V_{\text{heave}}/U_{\text{vertical}}$, were computed for each of

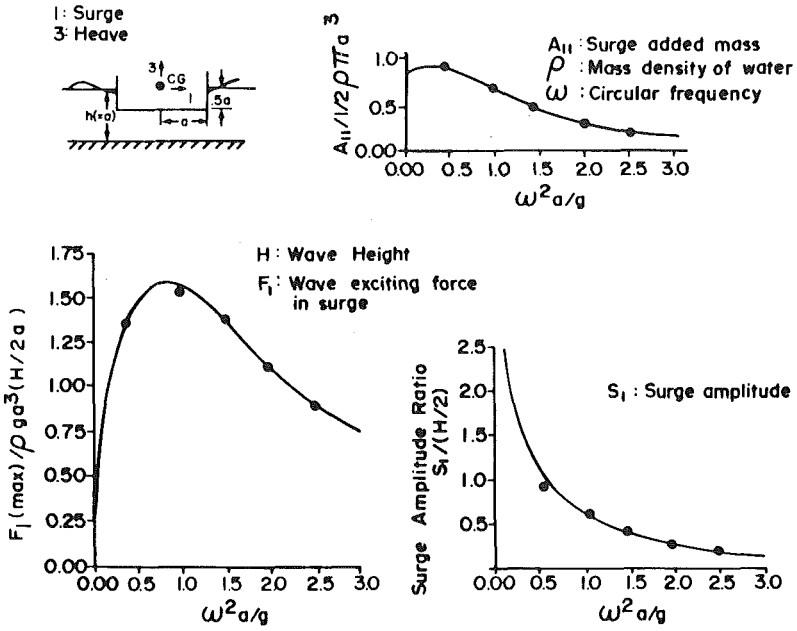


Fig. 1 Results for vertical circular cylinder in surge mode. Garrison [18], present results.

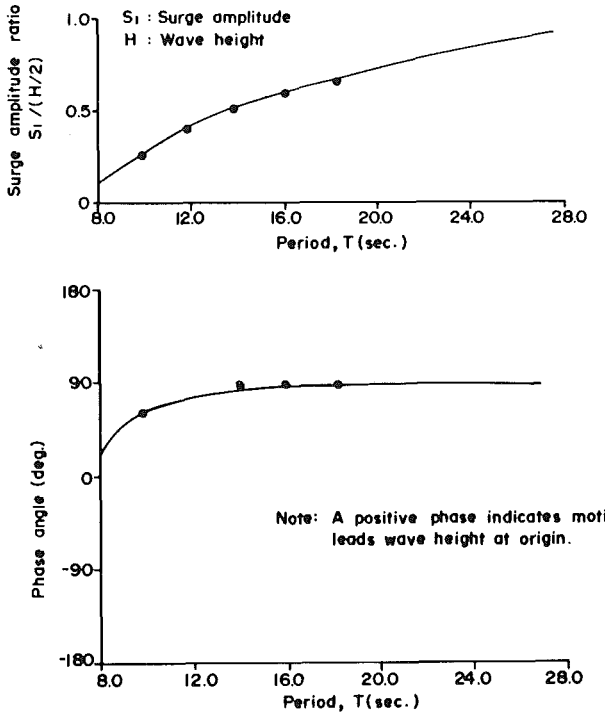


Fig. 2 Results for surge motion of a 90 × 90 × 20-m rectangular floating box. Present results, Faltinsen [17].

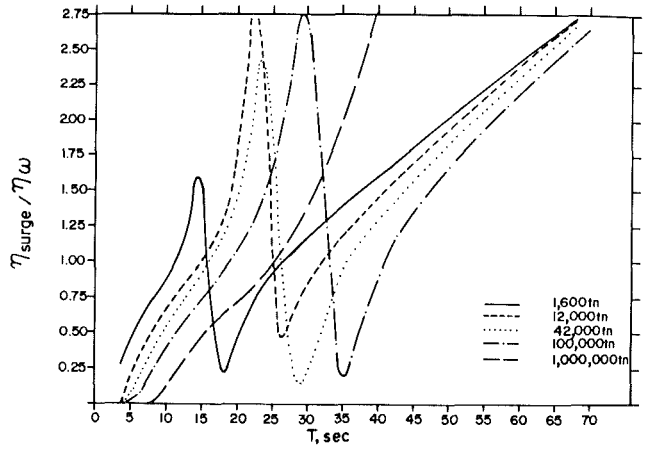


Fig. 3 Motion response in surge

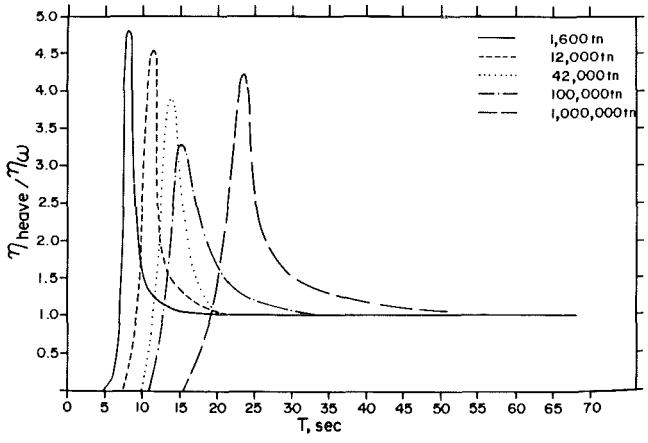


Fig. 4 Motion response in heave

the five model icebergs under study here. The particle velocity amplitudes were based on linear wave theory [16], to be consistent with the present theoretical formulation, viz,

$$U_{\text{horizontal}} = \frac{\pi H}{T}\coth\left(\frac{2\pi d}{\lambda}\right) \tag{1}$$

$$U_{\text{vertical}} = \pi H/T \tag{2}$$

$$T = \left\{\frac{2\pi\lambda}{g}\coth\left(\frac{2\pi d}{\lambda}\right)\right\}^{1/2} \tag{3}$$

where $d$ is the water depth and $\lambda$ is the wavelength.

The velocity ratios are plotted in Figs. 5 and 6 against $\lambda/L$, where $L$ is the length of a side, for each of the cubical iceberg models. For horizontal motion, the velocity ratios for all bergs tends towards 1.0 as $\lambda/L$ tends towards 10–14 (see Fig. 5). For larger values of $\lambda/L$, large scatter in the horizontal velocity

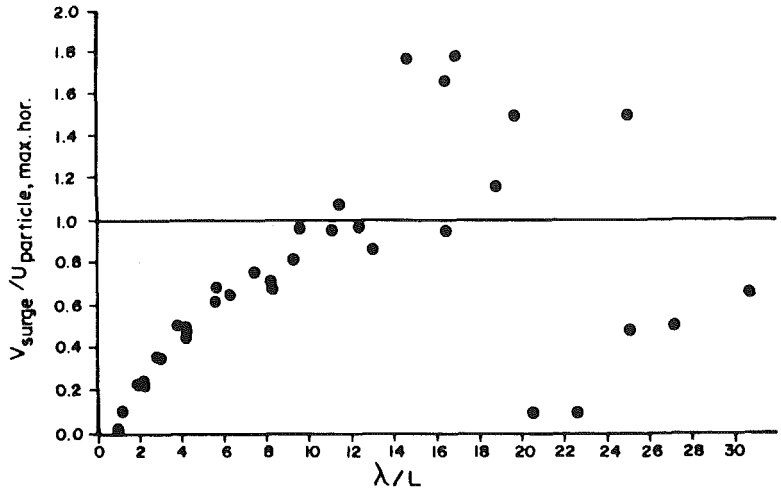


Fig. 5 Maximum horizontal velocity ratio

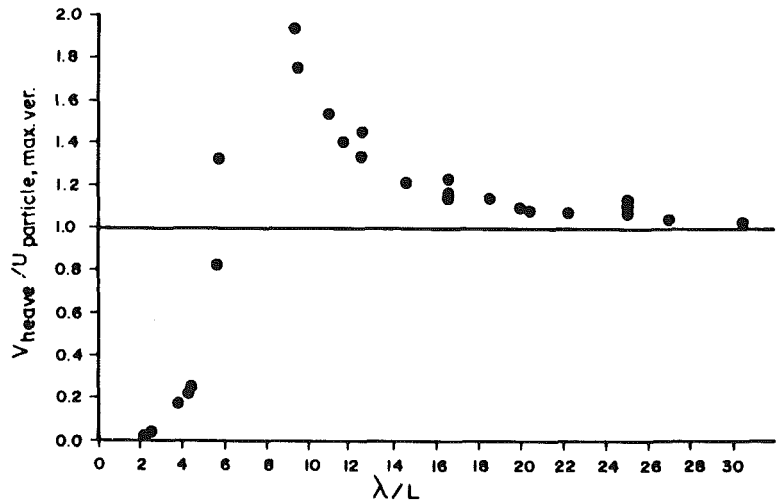


Fig. 6 Maximum vertical velocity ratio

ratio is seen. This is due to the nature of the surge RAOs (see Fig. 3), which each display a large peak followed by a sudden drop off for wave periods corresponding to $15 < \lambda/L < 25$. This behavior was not observed for the models tested in steep waves in reference [10].

The velocity ratios for vertical motion (see Fig. 6) overshoot unity in the range $6 < \lambda/L < 20$, tending towards unity for larger λ/L. The overshoot is due to the pronounced heave resonance response predicted by the present linear model. The actual response would undoubtedly be nonlinear for large-amplitude resonance motion, and would be limited by submergence of the bergs and fluid viscosity.

Keeping in mind the differences between the experimental tests in steep waves conducted by Lever, et al. [10], and the linear potential flow model presented here, the results are in general agreement. Icebergs should display fluid particlelike behavior (or at least move at maximum instantaneous velocities approaching fluid particle velocities) for $\lambda/L$ greater than 10–15.

**2.3 Response of Icebergs in Irregular Seas.** The unidirectional JONSWAP sea-spectrum was chosen as a reasonable representation of a North Atlantic wave energy distribution. This spectrum takes the form (from [25])

$$S_w(f) = \frac{A}{f^5}\exp(-B/f^4)\gamma^a \tag{4a}$$

where

$$a = \exp\{-(f - f_0)^2/(2\sigma^2 f_0^2)\}$$

$$\sigma = 0.07 \quad \text{for} \quad f \le f_0 \tag{4b}$$

$$\sigma = 0.09 \quad \text{for} \quad f > f_0 \tag{4c}$$

$$A = \frac{5\,H_s^2 f_0^4}{(16\gamma^{1/3})} \quad \text{for} \quad 1 < \gamma < 4 \tag{4d}$$

$$B = 5\,f_0^4/4 \tag{4e}$$

and where $f_0$ is the peak frequency in the spectrum, $H_s$ is the significant wave height, $\gamma$ is the peak enhancement factor. A constant value of $\gamma = 2.2$ was chosen, as this is the average value reported by LeBond, et al. [25] based on 36 wave spectra from the Hibernia area in 95-m water depth. Similarly, a simple relationship between $H_s$ and peak period, $T_p \equiv 1/f_0$, has been used; namely (from [25])

$$T_p = 4.43\,H_s^{1/2} \tag{5}$$

Thus the wave energy spectrum, $S_w(f)$, has been reduced to dependence on significant wave height only.

The motion and velocity response spectra, $S_m(f)$ and $S_v(f)$, respectively, may be obtained by applying linear analysis in

the frequency domain (see, for example [26]). Thus,

$$S_m(f) = S_w(f) \cdot H^2(f) \tag{6}$$

$$S_v(f) = 4\,\pi^2 f^2 s_w(f) \cdot H^2(f) \tag{7}$$

where: $H(f) \equiv \eta_i(f)/\eta_w$ is the RAO for motion in the desired mode; $\eta_i(f)$ is the amplitude of motion in $i$th mode (here, either heave or surge); $\eta_w$ is the wave amplitude. Thus, for a given iceberg model, $S_m(f)$ and $S_v(f)$ will also depend only on $H_s$.

The characteristic parameters of a given velocity response spectrum, such as the rms of the velocity amplitude, $V_{\text{rms}}$, the significant velocity (or average of highest ⅓ of velocity amplitudes), $V_s$, etc., may be estimated assuming the spectrum to be Rayleigh type. This assumption is usual practice in determining motion response of ships to narrow band irregular seas (see, for example, [26]), and yields

$$V_{\text{rms}} = \{2\ m_0\}^{1/2} \tag{8}$$

$$V_s = 2\{m_0\}^{1/2} \tag{9}$$

where $m_0$ is the zeroth moment of the velocity spectrum

$$m_0 = \int_0^\infty S_v(f)\ df \tag{10}$$

The use of equations (8) and (9) will yield accurate results provided the velocity spectra are narrow banded. This was found to be true in all cases and reflects the use of the sharp peaked JONSWAP spectra for $S_w(f)$.

The computed values of $V_s$ for surge and heave motion obtained for various values of $H_s$ are shown plotted in Figs. 7 and 8, respectively. The variation of $V_s$ with $H_s$ was found to be nearly linear for surge motion, with significant velocities for the 1600-tonne berg approaching 3 m/s in 10 m significant wave height seas. The response naturally decreases with increasing iceberg size. The heave motion response varies less linearly, due in part to the prominent heave resonance spike in the computed RAOs.

## 3 Influence of Wave-Induced Motion on Iceberg Velocity Probability Distribution

**3.1 Probability Density for Significant Surge Velocity.** Having obtained the relationship between $V_s$ and $H_s$ for each model iceberg (shown in Fig. 7 for surge), to determine the probability density for $V_s$, only the probability density for $H_s$ is required, $P_H(H_s)$. The 11-yr data compiled by Neu [27] for the Hibernia region were used. The probability density for $H_s$ was determined by combining all 8026 wave observations for the Hibernia region into a histogram and normalizing the result. Figure 9 shows $P_H(H_s)$ obtained in this way. The probability densities of surge $V_s$ for each berg, $P_s(V_s)$, determined by combining the curves from Fig. 7 with $P_H(H_s)$, are shown in Fig. 10.

It should be noted that the above method ignores monthly variations in $P_H(H_s)$ and iceberg population density. Since highest iceberg densities occur in April–May on the Grand Banks, and sea-state conditions during this period are approximately equal to the yearly average values, this omission should not affect the results significantly. The development of a full iceberg impact risk analysis would require consideration of monthly variations in iceberg population density and significant wave height at the site of interest.

**3.2 Probability Density for Mean Drift Speed.** It is standard iceberg management procedure to track all icebergs detected by the marine radar of an offshore drilling rig. The range and bearing of each target is normally recorded hourly. From this data, average hourly drift speed estimates may be obtained.

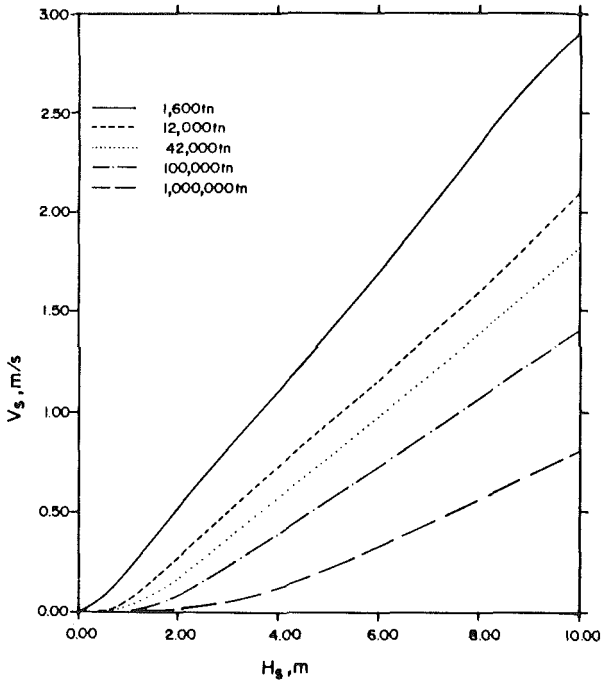


Fig. 7 Significant surge velocities at various sea-states

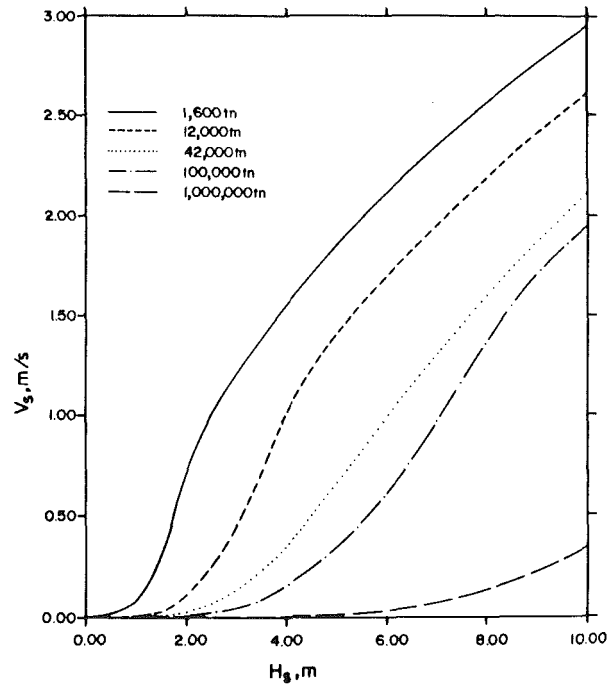


Fig. 8 Significant heave velocities at various sea-states

Although there is some evidence that small bergs drift more quickly than large ones, e.g., [9, 28], the correlation is not strong. Hence, it has been assumed that drift speed is independent of iceberg size. The data collected by Eastcan during the summer drilling seasons of 1975 and 1976 have been used [7, 8]. These consist of 2088 observations at four drill sites in the Labrador Sea. Other drift velocity statistics could be used, as the results will be similar. The probability density for drift speed, $P_d(V_d)$, is shown in Fig. 11 (drift alone curve).

**3.3 Total Velocity Probability Density.** The total velocity of an iceberg at any instant may conveniently be represented as the sum of the mean drift velocity plus the unsteady

velocity due to wave action. In principle, this would be a vector summation so that to properly add in wave-induced motion to mean iceberg drift, some account of wave versus drift direction would be required. To do this would require directional wave spectra and directional iceberg drift probability distributions. Even then, the influence of the structure on the behavior of the berg would not be taken into account.

For the purposes of risk analysis, a simpler approach is proposed. The total velocity, $V_t$, is taken to be the sum of the drift speed plus the significant surge velocity. That is,

$$V_t = V_d + V_s \tag{11}$$

This expression requires some elaboration.

Reasonable estimates of impact velocities are desired; ones which could be expected during iceberg/structure interactions. It has already been argued that mean drift speeds ignore potentially significant wave-induced iceberg motion. Consider then what would be recorded if existing radar technology permitted continuous readout of total instantaneous iceberg velocity. A 1-hr time history would essentially reproduce the mean drift speed, $V_d$, plus a fluctuating component whose magnitude and direction varied with time. For bergs as large as 200,000 tonnes, the second-order wave drift force can be as large as the sum of all other forces [14]. In addition, any wind which generates local waves also produces aerodynamic drag on the berg and a surface current drag along somewhat the same general direction. It is therefore not unreasonable that the fluctuating velocities might be centered on the mean drift direction, particularly for smaller bergs.

Note that, in a random sea with a peak period of 12 s (corresponding to $H_s = 7.3$ m, from equation (5)), the iceberg could encounter, and respond to, approximately 300 waves during the 1-hr observation period. $V_s$ would be the average of the highest 100 velocity fluctuations. Even accounting for directional effects, a total velocity of $V_d + V_s$ would likely be exceeded many times during the hour. Or, put another way, an iceberg drifting at a mean speed of 0.25 m/s would take approximately 400 s to traverse a 100-m drilling platform. In a random sea of 12-s peak period, $V_s$ would be the average of the highest 11 or so instantaneous iceberg surge velocities. Again, a total velocity of $V_d + V_s$ would likely be exceeded several times during the traverse period.

While the present formulation ignores the influence of the structure on the relative impact velocity, and mean drift and wave directional variations, it also ignores the possibility of repeated impacts. That is, if an impact occurs at a low relative velocity such that little damage occurs to the iceberg, the possibility still exists that a more energetic collision will take place before the iceberg clears the vicinity of the structure. Thus, in spite of its simplicity, it is felt that equation (11) gives an expression for the total velocity which reasonably represents the hazard an iceberg poses to an offshore structure, including the influence of ocean waves.

The probability density for total velocity may now be easily obtained by convolution; namely

$$P_t(V_t) = \int_0^{V_t} P_d(V_t - V_s) P_s(V_s)\, dV_s \tag{12}$$

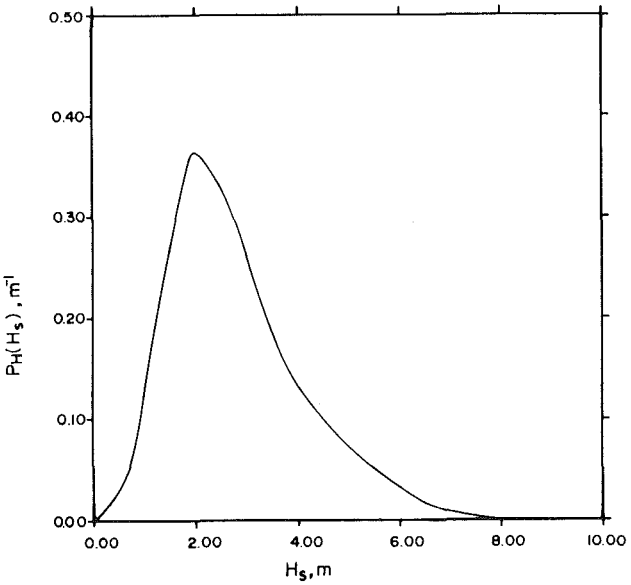


Fig. 9 Probability density of $H_s$ (full year) from data of Neu [27]

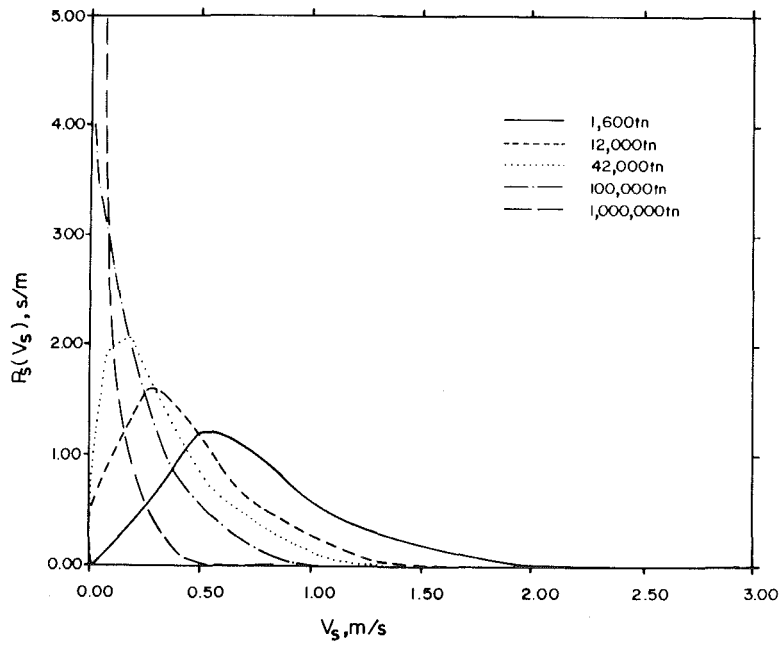


Fig. 10 Probability density of significant surge velocity

The results for all model icebergs considered are shown in Fig. 11, with the velocity exceedence levels shown in Fig. 12 and Table 1. Since iceberg kinetic energy is also used in some ice/structure interaction models, the corresponding total kinetic energy exceedence levels (exclusive of added mass) are shown in Table 2 for specific berg sizes.

## 4 Discussion

Careful scrutiny of the results shown in Figs. 11, 12 and Table 1 reveals that wave-induced motion represents a significant component of total iceberg motion, in a probabilistic sense. The responses of model icebergs to irregular seas have been combined with the probability of occurrence of each sea-state. The resulting total velocity probability densities or exceedence curves represent results that might actually have been measured in the field if appropriate technology existed to do so. The values would correspond to instantaneous iceberg velocities reached or exceeded many times during each 1-hr observation interval.

**Table 1 Exceedance levels, $E(V)$, for total velocity $V_t$ and drift velocity $V_d$**

| $E(V)$ (percent) | $V_t$, m/s (tonnes) | | | | | $V_d$, m/s |
|---|---|---|---|---|---|---|
| | 1600 | 12,000 | 42,000 | 100,000 | 1,000,000 | |
| 50 | 0.93 | 0.66 | 0.53 | 0.43 | 0.28 | 0.21 |
| 20 | 1.32 | 0.96 | 0.82 | 0.66 | 0.45 | 0.36 |
| 10 | 1.56 | 1.15 | 0.98 | 0.80 | 0.55 | 0.45 |
| 5 | 1.78 | 1.31 | 1.13 | 0.92 | 0.63 | 0.52 |
| 1 | 2.14 | 1.58 | 1.40 | 1.15 | 0.78 | 0.65 |

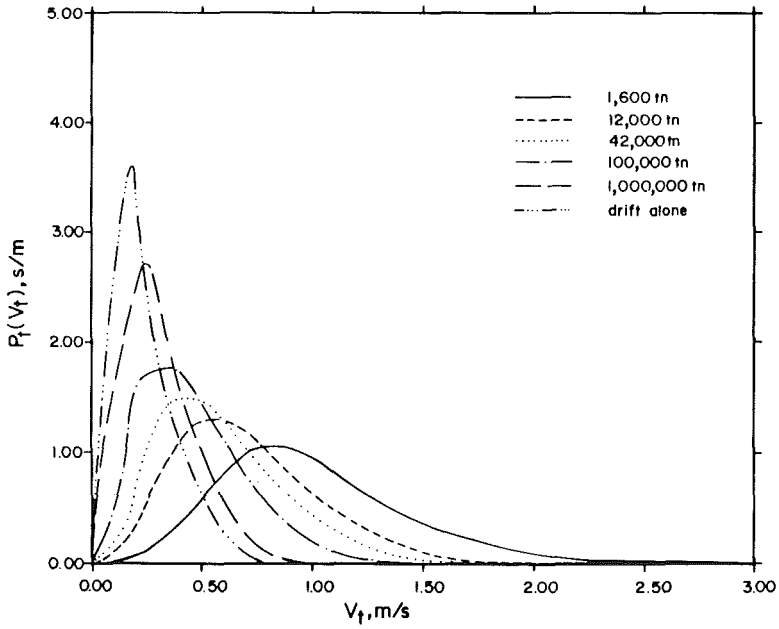


**Fig. 11 Probability density of total velocity**

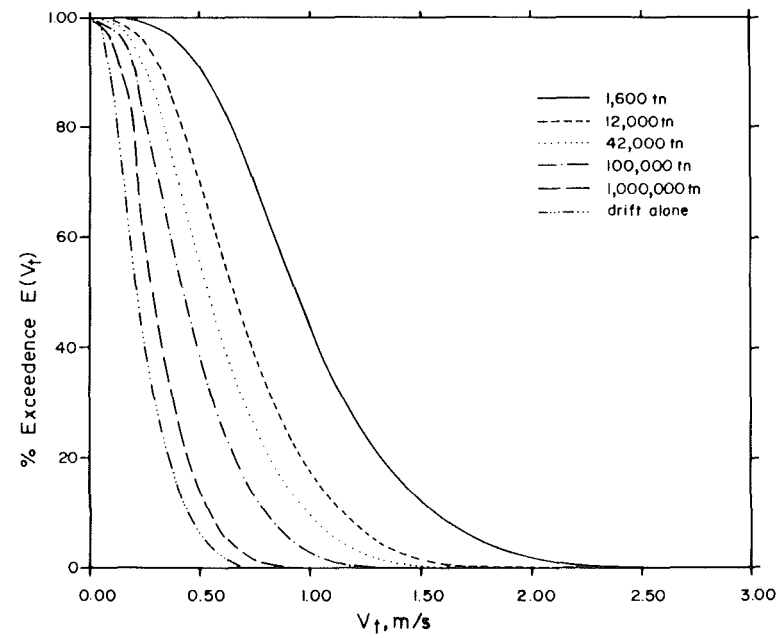


**Fig. 12 Total velocity exceedance curves**

Table 2 Kinetic energy of exceedance levels, $E(\frac{1}{2}MV^2)$, based on drift velocity along, $\frac{1}{2}MV_d^2$, and with wave effects included, $\frac{1}{2}MV_t^2$. Kinetic energy values in KJ.

| $E(\frac{1}{2}MV^2)$ (percent) | 1600 tonne | | | 12,000 tonne | | | 42,000 tonne | | | 100,000 tonne | | | 1,000,000 tonne | | |
|---|---|---|---|---|---|---|---|---|---|---|---|---|---|---|---|
| | $\frac{1}{2}MV_d^2$ | $\frac{1}{2}MV_t^2$ | Ratio | $\frac{1}{2}MV_d^2$ | $\frac{1}{2}MV_t^2$ | Ratio | $\frac{1}{2}MV_d^2$ | $\frac{1}{2}MV_t^2$ | Ratio | $\frac{1}{2}MV_d^2$ | $\frac{1}{2}MV_t^2$ | Ratio | $\frac{1}{2}MV_d^2$ | $\frac{1}{2}MV_t^2$ | Ratio |
| 50 | 37 | 669 | 18 | 292 | 2680 | 9 | 986 | 6510 | 7 | 2340 | 8960 | 4 | 23,800 | 40,500 | 1.7 |
| 20 | 101 | 1370 | 14 | 809 | 5910 | 7 | 2730 | 10,300 | 5 | 6470 | 21,400 | 3 | 65,800 | 101,000 | 1.5 |
| 10 | 156 | 1390 | 9 | 1250 | 8210 | 7 | 4200 | 19,900 | 5 | 9960 | 31,900 | 3 | 101,000 | 152,000 | 1.5 |
| 5 | 214 | 2460 | 11 | 1710 | 10,700 | 6 | 5770 | 26,900 | 5 | 13,700 | 42,300 | 3 | 139,000 | 202,000 | 1.5 |
| 1 | 317 | 3520 | 11 | 2610 | 15,400 | 6 | 8820 | 40,300 | 5 | 20,900 | 66,200 | 3 | 213,000 | 314,000 | 1.5 |

Naturally, the deviation between total velocity and drift velocity is found to be greatest for the smallest ice masses. The 1 percent exceedence velocity for a 1600-tonne growler was found to be 2.14 m/s, a 330 percent increase over the value based on drift velocity alone. By comparison, the 1 million-ton iceberg shows a much smaller, but still significant, 20 percent increase in its 1 percent velocity exceedence level, from 0.65 m/s to 0.78 m/s (see Table 1).

It is felt that the most useful result of the present work, however, is to show how drift velocity statistics can be systematically upgraded to include instantaneous motion over the entire range of iceberg sizes and seastates. The present approach should be compared with that of Johnson and Nevel [6] where the velocity exceedence curve is doubled, independent of iceberg mass. Note that the present systematic accounting for wave-induced motion predicts higher impact velocities for small ice masses, and lower impact velocities for large icebergs, for all exceedence levels, as compared with across the board doubling of velocities.

It is also interesting to note that the increases in kinetic energy exceedence values, for specific berg sizes, tend towards constant percentages for all five model icebergs (see Table 2). For 20 percent exceedence levels and higher, the ratios between total and drift kinetic energies for the 1600, 12,000, 42,000, 100,000, and 1,000,000-tonne bergs are approximately 10, 6, 5, 3, 1.5, respectively. That is, virtually all probable ice/structure impacts are likely to be substantially more energetic than estimates based on drift speed data alone would indicate.

The key assumptions used to produce these results bear repeating here: (*a*) the wave-induced motions of the iceberg models were computed using linear potential flow theory; (*b*) the total velocity was taken as the scalar sum of the drift speed with the significant surge velocity obtained for a unidirectional random sea.

The use of linear wave theory will tend to underpredict full-scale instantaneous velocities of the smaller ice masses in heavier seastates, as the required assumptions of nonsteep waves and small body motion are violated. The effect of fluid viscosity on the results is not expected to be as important.

Conversely, the scalar addition of $V_s$, obtained for unidirectional seas, to $V_d$ ignores the directional content of an irregular sea and differences between mean wave and drift directions. This shortcoming must be placed in context, however. The most appropriate set of iceberg velocity statistics would be one which described probable values of relative velocity likely to occur on impact of a berg with a structure. While in principle, thorough study of the complete wind/wave/current/ice/structure interaction could yield such results, this analysis would be extremely complicated. As it stands, existing risk analyses ignore the influence of the structure on iceberg motion and use open water drift velocities as input. The authors feel that the present approach extends this one step further to include wave-induced ice motion. Preliminary wave tank results available suggest that when iceberg/structure impacts do occur, the impact velocities are typically close to maximum velocities seen in open seaway conditions [10, 29]. While the wave/ice/structure interaction is undoubtedly important, it may be more effective for purposes of risk analyses to consider the influence of the structure on the wave field as a change in the target width seen by the berg [30].

Since a total velocity of $V_s + V_d$ would likely be reached or exceeded several times during a 1-hr observation, or for the duration that an iceberg might pose a threat to a structure, the authors believe this value is a realistic choice of input velocity for risk analysis based design models. Although the quantitative results would change, the use of a velocity level lower than $V_s$ to represent instantaneous velocity effects could easily be incorporated into the method, and would not substantially change the conclusion that wave-induced motion should be taken into account. Work underway at C-CORE/MUN to measure full-scale, wave-induced iceberg motion should help to clarify this matter.

## 5 Conclusions

A systematic method has been developed, based on three-dimensional potential flow theory, to upgrade iceberg velocity statistics to include wave-induced motion. The results indicate that instantaneous rather than drift velocity data should be used for all bergs under 1 million tonnes. Remarkably, icebergs in the 10,000–100,000-tonne range can be expected to have instantaneous impact kinetic energies 3–6 times higher than the corresponding levels based on drift speed alone.

Work is presently underway to study and quantify the importance of wave effects on ice/structure interactions in much greater detail. Full-scale data are being obtained to verify open seaway model tests; a study into the importance of nonlinear wave effects and large ice motion is underway; the response of icebergs in multi-directional seas is under study; and several wave tank investigations into the influence of the structure on nearby ice motion have been initiated. It is hoped that this effort will improve our understanding of wave/ice/structure interactions substantially, and lead to safe and economical designs for structures exposed to possible iceberg impact.

## Acknowledgments

The authors gratefully acknowledge the financial support of the National Sciences and Engineering Research Council of Canada, and Imperial Oil Ltd.

## References

1 Arockiasamy, M., Reddy, D. V., and Muggeridge, D. B., "Dynamic Responses of Moored Semisubmersibles in an Ice Environment," Structures Congress, ASCE, Houston, Preprint SC-12, 1983.

2 Cammaert, A. B., Wong, T. T., and Curtis, D. D., "Impact of Icebergs on Offshore Gravity and Floating Platforms," *POAC '83*, Helsinki, 1983, pp. 519–536.

3 Kitami, E., et al., "Iceberg Collision with Semi-submersible Drilling Unit," *IAHR Symposium*, Hamburg, 1984, pp. 45–53.

4 Maes, M. A., Jordaan, I. J., Appleby, J. R., and Fidjestøl, P., "Risk Assessment of Ice Loading for Fixed Structures," *3rd International Conference on Offshore Mechanics and Arctic Engineering*, New Orleans, Vol. III, 1984, pp. 220–277.

5 Nessim, M. A., Murray, A., Maes, M. A., and Jordaan, I. J., "Risk Analysis Methodology for Mobil Offshore Units Operating in Ice-Infested Waters," *Ice Tech '84, 3rd International Conference on Icebreaking and Related*

*Technologies*, SNAME, 1984, pp. H1–H12.

6 Johnson, R. C., and Nevel, D. E., "Ice Impact Structural Design Loads," *POAC '85, 8th International Conference on Port and Ocean Engineering under Arctic Conditions*, Narssarssuaq, Vol. 2, Sept. 1985, pp. 569–578.

7 Marex Marine Environmental Services Ltd., "Offshore Labrador 1976," Summary Report prepared for Total Eastcan, 1977.

8 Marex Marine Environmental Services Ltd., "Offshore Labrador 1975," Summary Report prepared for Total Eastcan, 1976.

9 Marex Marine Environmental Services Ltd., "Iceberg Observations," Offshore Laborador—Appendix 3, Iceberg Observations D.V. Sedco 445, 1975.

10 Lever, J. H., Reimer, E., and Diemand, D., "A Model Study of the Wave-Induced Motion of Small Icebergs and Bergy Bits," *3rd International Symposium on Offshore Mechanics and Arctic Engineering*, Vol. III, 1984, pp. 282–290.

11 Kristensen, M., and Squire, V. A., "Modelling of Antarctic Icebergs in Ocean Waves," *Annals of Glaciology*, Vol. 4, 1983.

12 Squire, V. A., "Numerical Modelling of Realistic Ice Floes in Ocean Waves," *Annals of Glaciology*, Vol. 4, 1983, pp. 277–282.

13 Squire, V. A., "Numerical Simulation of Ice Floes in Waves," Scott Polar Research Institute, Sea Ice Group, Technical Report 81-1, 1981.

14 Hsiung, C. C., and Aboul-Azim, A. F., "Iceberg Drift Affected by Wave Action," *Ocean Engineering*, Vol. 9, No. 5, 1982.

15 Lever, J. H. and Diemand, D., "Measurement of Instantaneous Motions of Ice Masses at Sea: 1984 Pilot Program," *POAC '85, 8th International Conference on Port and Ocean Engineering under Arctic Conditions*, Greenland, Vol. 2, Sept. 1985, pp. 988–997.

16 Sarpkaya, T., and Issacson, M., *Mechanics of Wave Forces*, Van Nostrand Co., 1981.

17 Faltinsen, O. M., and Michelsen, F. C., "Motion of Large Structures in Waves at Zero Froude No.," *International Symposium on Dymamics of Marine Vehicles and Structures in Waves*, London, 1974, pp. 91–106.

18 Garrison, C. J., "Hydrodynamics of Large Objects in the Sea, Part II: Motion of Free Floating Bodies," *Journal of Hydronautics*, Vol. 9, No. 2, 1975, pp. 58–63.

19 Salvasen, N., Tuck, E. O., and Faltinsen, O. M., "Ship Motions and Sea Loads," *Trans. of SNAME*, Vol. 78, 1970, pp. 250–287.

20 Kim, W. D., "On the Harmonic Oscillation of a Rigid Body on a Free Surface," *Journal of Fluid Mechanics*, Vol. 21, Part 3, 1965, pp. 427–451.

21 Hsiung, C. C., Sen, D., and Tse, C. C., "Floating Production System: Hydrodynamics Analysis and Model Testing," Technical Report to CanOcean Ltd., Memorial University of Newfoundland, 1983.

22 Nojiro, N., "A Study of Hydrodynamic Pressures and Wave Loads on Three-Dimensional Floating Bodies," *IHI Engineering Review*, Vol. 14, No. 2, 1981, pp. 6–20.

23 Pinkster, J. A., and Van Oortmerssen, G., "Computation of the First and Second Order Wave Forces on Bodies Oscillating in Regular Waves," *Proceedings of the 2nd International Conference on Numerical Ship Hydrodynamics*, University of California, Berkeley, 1977, pp. 136–156.

24 Sen, D., "Prediction of Wave Loads and Motions of Floating Marine Structures by 3-Dimensional Flow Theory," Masters thesis, Memorial University of Newfoundland, 1983.

25 LeBlond, P. H., Calisal, S. M., and Isaacson, M., "Wave Spectra in Canadian Waters," Canadian Contract Report of Hydrography and Ocean Sciences.

26 Bhattacharyya, R., *Dynamics of Marine Vehicles*, Wiley, New York, 1978.

27 Neu, H. J. A., "11-Year Deep Water Wave Climate of Canadian Atlantic Waters," Canadial Technical Report of Hydrography and Ocean Sciences, No. 13, 1982.

28 Wright, B., and Beranger, D., "Ice Conditions Affecting Offshore Hydrocarbon Production in the Labrador Sea," *International Conference*, Hamburg, 1980, pp. 390–402.

29 El-Tahan, H., Arockiasamy, M., and Swamidas, A. S. J., "Motion and Structural Response of a Hydroelastic Semi-submersible Model to Waves and Ice Impacts," *4th International Symposium on Offshore Mechanics and Arctic Engineering*, Vol. I, 1985, pp. 753–761.

30 Lever, J. H., and Raisanen, P., "Development of a 3-D Wave Diffraction Model for Bergy Bit Motion in the Vicinity of a Drillship," in preparation.